室蘭工業大学
学術資源アーカイブ
Muroran Institute of Technology Academic Resources Archive

On the Distributed Coupled-Line Digital Frequency Multipliers -Part Ⅰ: the Frequency Domain Behaviour

メタデータ	言語: English 出版者: 室蘭工業大学 公開日: 2014-03-04 キーワード (Ja): キーワード (En): 作成者: 坂上, 岩太 メールアドレス: 所属:
URL	http://hdl.handle.net/10258/770

On the Distributed Coupled-Line Digital Frequency Multipliers – Part I: the Frequency Domain Behaviour

Iwata SAKAGAMI

Abstract

Functions of coupled-line type digital frequency multipliers are described from the aspect of frequency domain by using Fourier transforms. Discrete frequency components of both a train of periodical impulses and that of pulses are firstly introduced. It has been shown that the proposed multipliers act as a kind of passive filter, that is, certain discrete frequency components are eliminated and others are passed. Secondly, this paper has proved that the attenuation of the transmitted components is minimized in the frequency characteristics of coupled-line type multipliers. Lastly, referring to a train of Gaussian pulses, it has been demonstrated that the proposed multipliers can function well under the network transfer functions based on TEM wave approximations.

I. Introduction

The multiplication of pulse repetition frequencies in the microwave frequency bands distributed coupled-line networks has been reported, and experiments have shown good agreement with the predictions of network systhesis theory[1], [2]. In the process of network systhesis, it has been convenient to treat a train of input pulses as a train of impulses. This is so that the principle of the coupled-line type multipliers can be understood easily, and because the output responses from arbitrary input waveforms can be obtained by the convolution integral[3].

The train of impulses possesses equi-amplitude equi-spacing discrete frequency components over $-\infty < \omega < \infty$, but no problems crop up as far as the network transfer functions are concerned. Expressed by the delay oprator z^{-1} or the Richards variable $t = j\tan\theta$, the network transfer functions have periodical frequency characteristics at all frequencies of $-\infty < \omega < \infty$. Therefore, conditions for the multiplication of the periodical impulses can be satisfied.

In general, the frequency characteristics in actual networks will show good agreement with those of the network transfer functions at the first or second period. However, as the frequency increases, the frequency characteristics stray from those of network transfer functions by the parasitc reactances at discontinuity interfaces or by conductor dielectric losses. Therefore, a pulse of finite duration should be introduced in real inputs and real networks as discussed at following sections.

The main topics here are: (i) discrete frequency components of periodical impulses, (ii) those of periodical pulses of finite duration, (iii) behavior of the proposed multipliers in the frequency domain, (iv) verification on the minimum insertion loss of the transmitted discrete frequency components, and (v) a train of Gaussian pulses.

II. Frequency Components of a Train of Input Pulses

(i) Discrete frequency components of periodical impulses.

Fig.1(a) shows the constant-resistance n-section coupled-line network. Figs.1(b)(c) are the equivalent circuits. They are similar to Figs.4(b)(c) in [2], differing in the position of b_i. Fig.1 will be explained in section IV again. Refs.[1,2] have shown three kinds of multipliers with regard to Fig.1(a). Figs. 2, 3 and 4 are the most simple input/output responses. They are realized by 1-section and 2-section networks in Fig.1(a).

In general, a train of unipolar impulses and a train of bipolar impulses are represented by[4]

$$a_n^+(t)=\sum_{k=-\infty}^{\infty}\delta(t-kT) \tag{1a}$$

$$a_n^+(t)=\sum_{k=-\infty}^{\infty}(-1)^k\delta(t-kT) \tag{1b}$$

The Fourier transforms of (1) are

$$\mathcal{F}[a_n^+(t)]=\omega^+\sum_{k=-\infty}^{\infty}\delta(\omega-k\omega^+) \tag{2a}$$

$$\mathcal{F}[a_n^-(t)]=\omega^+\sum_{k=-\infty}^{\infty}\delta\{(\omega-\frac{(2k+1)\omega^+}{2}\} \tag{2b}$$

where $\omega^+=2\pi/T$. T is the impulse interval. Although the period of (1a) is T, that of (1b) is treated as 2T in this paper. When eqs.(1) are applied to port A_1 in Fig.1(a), T must be $T=2(n+1)\tau$, where τ is a time delay in the line length ℓ.

The transient responses will be over in several nanoseconds in distributed networks of microwave frequency bands[5]. Therefore let eqs.(1) be incident impulse trains covering $-\infty<t<\infty$. In (1), it is assumed that a positive polarity impulse comes to port A_1 at $t=0$. Eqs.(2) show that the unit 1 $\pm$1 1 $\pm$1 impulse trains possess discrete frequency components of equi-amplitude ω^+ and equi-spacing ω^+

(ii) Discrete frequency components of periodical unipolar pulses.

Now let us consider a train of pulses v_{Tr} (t) [for instance, see Fig.5]. It is assumed that the constituent single pulse v(t) is time-limitted and the duration is less than 2π in order that the pulses not overlap at output port A_2. Designating the Fourier transform of v(t) by $V(\omega)$,

$$v(t)=\frac{1}{2\pi}\int_{-\infty}^{\infty}V(\omega)\exp(j\omega t)d\omega \tag{3a}$$

$$V(\omega)=\int_{-\infty}^{\infty}V(t)\exp(-j\omega t)dt \tag{3b}$$

Let t_0 be an arbitrary real number. As v(t) can be expressed as a linear combination of $\exp(jk\omega^+ t)$ on interval (t_0, t_0+T), the linear combination of v_{Tr} (t) holds on $(-\infty<t<\infty)$.

$$v_{Tr}(t)=\sum_{k=-\infty}^{\infty}V_k(k\omega^+)\exp(jk\omega^+t), \qquad (-\infty<t<\infty) \tag{4a}$$

$$V_k(k\omega^+)=\frac{1}{T}\int_{-T/2}^{T/2}v(t)\exp(-jk\omega^+t)dt \tag{4b}$$

Using (3b), (4b) and an assumption that v(t) is zero on $|t|>T/2$,

$$V_k(k\omega^+)=V(k\omega^+)/T \tag{5}$$

Therefore (4a) and the Fouier transform are

$$v_{Tr}(t)=\frac{1}{T}\sum_{k=-\infty}^{\infty}V(k\omega^{+})\exp(jk\omega^{+}t),\qquad(-\infty<t<\infty)\tag{6a}$$

$$\mathcal{F}[v_{Tr}(t)]=\omega^{+}\sum_{k=-\infty}^{\infty}V(k\omega^{+})\,\delta(\omega-k\omega^{+})\tag{6b}$$

Thus, the Fourier series expansion of periodic pulses can be obtained by using the Fourier transform of single pulse v(t). It is seen that (6b) is given by the product of (2a) and $V(\omega)$

(iii) Discrete frequency components of periodical pulses.

Let us consider the periodical bipolar pulses [for instance, see Fig.6] When w(t) consists of positive single pulse v(t) and negative single pulse $-v(t-T)$,

$$w(t)=\begin{cases}v(t]-v(t-T), & (-t_0\leq t\leq 2T-t_0)\\ 0 & ,\ (t<-t_0,\ t>2T-t_0)\end{cases}\tag{7a}$$

$$W(\omega)=\mathcal{F}[w(t)]=V(\omega)\{1-\exp(-j\omega T)\}\tag{7b}$$

Let a train of bipolar pulses consisting of w(t) be $w_{Tr}(t)$, and the period be 2T. Similarily to (4a) and (4b),

$$w_{Tr}=\sum_{k=-\infty}^{\infty}W_K(k\omega^{+}/2)\exp(jk\omega^{+}t/2),\qquad(-\infty<t<\infty)\tag{8a}$$

$$W_K(k\omega^{+}/2)=\frac{1}{2T}\int_{-t_0}^{2T-t_0}w(t)\exp(-jk\omega^{+}/2)dt\tag{8b}$$

At $-t_0\rightarrow-\infty$, $2T-t_0\rightarrow\infty$ in (8b),

$$W_K(k\omega^{+}/2)=W(k\omega^{+}/2)/2T,\tag{9}$$

From (7b),

$$W_K(k\omega^{+}/2)=\begin{cases}0 & (\text{k:even number})\\ V(kw^{+}/2)/T & (\text{k:odd number})\end{cases}\tag{10}$$

Therefore $w_{Tr}(t)$ and the Fourier trasform are written by

$$w_{Tr}(t)=\frac{1}{T}\sum_{k=-\infty}^{\infty}V\{(2k+1)\omega^{+}/2\}\exp\{j(2k+1)\omega^{+}t/2\},\qquad(-\infty<t<\infty)\tag{11a}$$

$$\mathcal{F}[w_{Tr}(t)]=\omega^{+}\sum_{k=-\infty}^{\infty}V\{\frac{(2k+1)\omega^{+}}{2}\}\,\delta\{\omega-\frac{(2k+1)\omega^{+}}{2}\}\tag{11b}$$

Similarily to the results of (6b), the train of periodical bipolar pulses can be represented using the Fourier transform $V(\omega)$, and (11b) is equal to the product of (2b) and $V(\omega)$.

III. Behavior of the Coupled-Line Type Multipliers in the Frequency Domain

(i) The case of faster unipolar pulses of time interval 2τ being output from input unipolar pulses of time interval $2(n+1)\tau$.

The examples of this case (i) are given by Fig.10 in [1], Figs.2(a)(b)and Figs.3(a)(b).

The network transfer function of Fig.1(a) is written as [1],[2]

$$\Gamma_n(z)=\sum_{k=0}^{n}q_kz^{-k}/\{1+\sum_{k=1}^{n}p_kz^{-k}\}\tag{12}$$

where $z^{-1}=\exp(-2j\omega\tau)$.

The condinions for the faster unipolar output impulses and output amplitude S_d were described in (22) of [1]. Using the same notations as in [2],

$$q_0=q_1=\ldots=q_n,\tag{13a}$$

$$S_d = q_0 / \{1 + \sum_{k=1}^{n} p_k\} \tag{13b}$$

Let the numerator of (12) be $f_2(z^{-1})$. From (13a),

$$f_2(z^{-1}) = q_0\ (1 + z^{-1} + \ldots + z^{-n})$$

Here $(1 - z^{-1}) f_2(z^{-1}) = q_0 \{1 - z^{-(n+1)}\}$ holds. Using $\omega^+ = \pi / (n+1)\tau$, the transmission zeros and their angular frequencies are given by

$$z_k = \exp\{j2\pi k/(n+1)\} = \exp\{2j(k\omega^+)\tau\} \tag{14a}$$

$$\omega_k = k\omega^+ \tag{14b}$$

where $k \neq m(n+1)$; k,m: integer.

Comparing (14b) with (2a) and (6b), it is seen that discrete frequency components of input unipolar impulse trains (or pulse trains) correspond to network transmission zeros, except for the case of $k = m(n+1)$. Therefore, the penetration of input impulse trains (or pulse trains) arises at $k = m(n+1)$. From (14b) and $T = 2(n+1)\tau$, the transmitted angular frequency components can be given by

$$\omega_t = m\pi / \tau. \tag{15}$$

(15) is equivalent to $z = 1$. One period of (12) corresponds to one turn on the unit circule of z-plane, that the insertion loss at (15) is constant.

$$\Gamma_n(z^{-1}) \mid_{z=1} = (n+1)Sd \tag{16}$$

Referring to (2a), as the amplitude is ω^+, the amplitude of transmitted frequency components is given by

$$\omega^+(n+1)S_d = \pi S_d / \tau \tag{17}$$

By (15) and (17), the discrete output responses in the frequency domain can be written as

$$\frac{\pi}{\tau} S_d \sum_{m=-\infty}^{\infty} \delta\left(\omega - \frac{m\pi}{\tau}\right) \tag{18}$$

This equation also represents the Fourier transform of an output unipolar impulse train of time interval 2τ

Fig.7 shows the transmitted frequency characteristics of Fig.9 in [1]. The center frequency f_0 was 192[MHz]. About 4 periods of the frequency characteristics are photographed. According to II(ii), because $\omega^+ = 2\pi f_0$, the discrete frequency components of the input unipolar pulse train which was given by Fig.10(a) in [1] are located just at frequencies of the maximum and minlmum attenuation. The discrete frequency components at the maximum attenuation are rejected, and those of minimum are transmitted to the output port along with network insertion losses. In this way, the resultant output pulse train become twice as fast as input one.

Ref.[2] has shown two other functions:

(ii) The case of faster bipolar pulses of time interval 2τ being output from input unipolar pulses of time interval $2(n+1)\tau$.

The input and output relations in Figs.2(a)(c) of this paper and Figs.8(a)(b) of [2] are the examples of this case(ii).

The realization conditions and the output amplitude S_p were given in (14) of [2].

$$q_0 = -q_1 = q_2 = \ldots = -q_n \tag{19a}$$

$$S_t = q_0 / \{1 + \sum_{k=1}^{n} (-1)^k p_k\} \tag{19b}$$

n:odd number

Further explanations of this case will be omitted.

(iii) The case of faster bipolar pulses of time interval 2τ being output from input bipolar pulses of time interval $2(n+1)\tau$.

Figs.8(b)(c) in [2] and Fig.4 of this paper are the example of this case (iii).

The frequency domain behaviours will be described below, although the discussions are similar to cases of (i) and (ii).

The realization conditions and the output amplitude S_p were given in (22) of [2].

$$q_0=-q_1=q_2=\ldots=q_n \tag{19a}$$

$$S_p=q_0/\{1+\sum_{k=1}^{n}(-1)^k p_k\} \tag{19b}$$

n:even number

As the numerator of (12) is given by $f_2(z^{-1})=q_0(1-z^{-1}+z^{-2}-\ldots+z^{-n})$, $(1+z^{-1})f_2(z^{-1})=q_0\{1+z^{-(n+1)}\}$ holds. Therefore the transmission zeros and the anglar frequencies are

$$z_k=\exp\{j(2k+n+1)\pi/(n+1)\}=\exp\{2j\cdot\frac{(2k+n+1)\pi}{2(n+1)\tau}\cdot\tau\} \tag{20a}$$

$$\omega_k=(2k+n+1)\omega^+/2 \tag{20b}$$

$k\neq m(n+1)$; k,m: integer

Comparing (20b) with (2b) and (11b), it will be understood that the discrete frequency components of input bipolar impulse trains (or pulse trains) coincide with network transmission zeros, except for the case of $k=m(n+1)$. Therefore, the peneration occurs at $k=m(n+1)$. The transmitted angular frequency components can be given by

$$\omega_t=(2m+1)\pi/2\tau \tag{21}$$

(21) corresponds to $z=-1$, and the insertion loss at (21) is

$$\Gamma_n(z^{-1})\mid_{z=-1}=(n+1)Sp \tag{22}$$

Since the amplitude of (2b) is ω^+,

$$\omega^+(n+1)S_p=\pi S_p/\tau \tag{23}$$

Thus, the discrete output responses in the frequency domain can be written by

$$\frac{\pi}{\tau}S_p\sum_{m=-\infty}^{\infty}\delta\{\omega-\frac{(2m+1)\pi}{2\tau}\} \tag{24}$$

(24) represents the Fourier transform of an output bipolar impulse train of time interval 2τ.

Fig.8 shows thoeretical frequency characteristics of 2-section coupled line digital frequency triplers. The solid curve and the chain curve indicate the cases of (i) and (iii), respectively. In the case of chain curve, the input bipolar impulse train possesses the normalized discrete frequency components 1/3, 1, 5/3 in the first period of $0\leq f/f_0<2$. The frequency components 1/3 and 5/3 are rejected by the network, and the frequency components $f/f_0=1$ transmits to output port. The transmitted frequency components are ±1, ±3, ±5, . . . at all frequency bands, and these components will form a three times faster impulse train than input.

The reader may wonder whether the distributed line networks could not satisfy the specified frequency characteristics at all frequencies, since the network transfer functions are based on the TEM wave approximations, and moreover the train of impulses is not an actual one. However, this question is answered in the light of (2), (6b) and (11b). In the case of a pulse train whose consti-

tuent pulses have finite duration, the amplitudes of discrete frequency components are determined by $\omega^{+}V(\omega)$. In general, the Fourier transform $V(\omega)$ of single pulse v(t) converges to zero as the frequency increases. Therefore if the energy of input pulse trains concentrates on the region of the specified frequency characteristics being satisfied, the proposed multipliers function well [See last section VI].

IV. The Non-Negative Constant

In this section, the non-negative constant will be taken up in preparation for discussion of the minimum instraction loss in the next section. The non-negative constant is occasionally used in the synthesis of cascaded transmission line networks[6],[7]. The phasical nature will be clarified.

Let us start at different derivations of network transfer functions from (3) and (4) in [2]. The reflection and transmission coefficients of the network shown in Fig.1(a) are defind as

$$\Gamma_n(z^{-1})=b_0/a_0 \tag{25a}$$

$$T_n(z^{-1})=c_\ell/a_0 \tag{25b}$$

(25a) is the same as network transfer function from port A_1 to port A_2.

In Figs.1(b)(c), the a_0, b_0, a_1, b_1, . . ., a_n, b_n, c_ℓ are the power waves[8]. The r_{ei} and t_{ei} ($i=1,2,\ldots,n+1$) are defined in the same way as in [1,2] and represent the reflection transmission coefficients at the ith interface. Paying attention to the a_m, b_m, a_{m+1}, b_{m+1} at the $(m+1)$ −section in Fig.1(b) or (c),

$$\begin{bmatrix} z^{-1}a_m \\ z^{-1/2}b_m \end{bmatrix} = \frac{1}{t_{e,m+1}} \begin{bmatrix} 1 & r_{e,m+1}z^{-1} \\ r_{e,m+1} & z^{-1} \end{bmatrix} \begin{bmatrix} z^{-1/2}a_{m+1} \\ b_{m+1} \end{bmatrix}$$

Therefore the relation of a_1, b_1, a_n, b_n, is given by

$$\begin{bmatrix} z^{-n/2}a_1 \\ z^{-(n-1)/2}b_1 \end{bmatrix} = \frac{1}{\mu'} \left\{ \prod_{m=2}^{n} \begin{bmatrix} 1 & r_{em}z^{-1} \\ r_{em} & z^{-1} \end{bmatrix} \right\} \begin{bmatrix} z^{-1/2}a_n \\ b_n \end{bmatrix} \tag{26}$$

where $\mu'=(t_{e2}t_{e3}\ldots t_{en})$.

On a_0, b_0, a_1, b_1 at first section,

$$\begin{bmatrix} z^{-(n+1)/2}a_0 \\ z^{-(n+1)/2}b_0 \end{bmatrix} = \frac{1}{t_{e1}} \begin{bmatrix} 1 & r_{e1}z^{-1} \\ r_{e1} & z^{-1} \end{bmatrix} \begin{bmatrix} z^{-n/2}a_1 \\ z^{-(n-1)/2}b_1 \end{bmatrix}$$

At the place of conductance g_1,

$$\begin{bmatrix} z^{-1/2}a_n \\ b_n \end{bmatrix} = \frac{z^{-1/2}c_\ell}{t_{e,n+1}} \begin{bmatrix} 1 \\ r_{e,n+1} \end{bmatrix}$$

These conditions lead (26) to

$$\begin{bmatrix} z^{-(n+1)/2}a_0 \\ z^{-(n+1)/2}b_0 \end{bmatrix} = \frac{z^{-1/2}c_\ell}{\mu} \left\{ \prod_{m=1}^{n} \begin{bmatrix} 1 & r_{em}z^{-1} \\ r_{em} & z^{-1} \end{bmatrix} \right\} \begin{bmatrix} 1 \\ r_{e,n+1} \end{bmatrix} \tag{27}$$

where $\mu=(t_{e1}t_{e2}\ldots t_{e,n+1})$.

Calculating the matrices inside the $\{\}$, the resultant elements $f_1(z^{-1})$ and $f_2(z^{-1})$ are n-th order polinomials of z^{-1} whose coefficient of each term is composed of products and sums of r_{em}($m=1,2,\ldots,n$). Therefore, (27) can be rewritten as

$$\begin{bmatrix} z^{-(n+1)/2}a_0 \\ z^{-(n+1)/2}b_0 \end{bmatrix} = \frac{z^{-1/2}c_\ell}{\mu} \begin{bmatrix} f_1(z^{-1}) \\ f_2(z^{-1}) \end{bmatrix} \tag{28}$$

From (25) and (28),

$$\Gamma_n(z^{-1})=f_2(z^{-1})/f_1(z^{-1}) \tag{29a}$$
$$T_n(z^{-1})=\mu z^{-n/2}/f_1(z^{-1}) \tag{29b}$$

In Fig.1(b), regarding the even mode cascaded transmission-line(EMCTL) between $1-1_1$ and $(n+1)-(n+1)_1$ as a black-box, a_0, b_0 and c_ℓ respectively represent the incident, reflected and transmitted power waves of the black-box. As the conductance g_1 is not inculded and the EMCTL is lossless, $|a_0|^2=|b_0|^2+|c_\ell|^2$. Therefore, from (25) and (29),

$$f_1(z^{-1})f_1^*(z^{-1})-f_2(z^{-1})f_2^*(z^{-1})=\mu^2 \tag{30}$$

$*$: complex conjugate

In this way, it has been demonstrated that the non-negative constant stated in [6],[7] is given by the square of the product of the transmission coefficient at the discontinuity interface of each unit element.

V. The Minimum Insertion Losss

According to three capabilities as digital frequency multipliers, the numerators of (29a) are given by

(i) $f_2(z^{-1})=q_0(1+z^{-1}+\ldots+z^{-n})$

(ii) $f_2(z^{-1})=q_0(1-z^{-1}+\ldots-z^{-n})$

n:odd number

(iii) $f_2(z^{-1})=q_0(1-z^{-1}+\ldots+z^{-n})$

n:even number

Values of the above-mentioned three equations are respectively equal to

$$f_2(z^{-1})\,|_{z=\pm1}=q_0(n+1) \tag{31}$$

at $z=1, -1, -1$. Here $q_0=r_{e1}$, and $0<r_{e1}<1$ holds as r_{e1} represents a reflection coefficient at the discontinuity interface $1-1_1$ in Fig.1(b). Taking the triangle inequality to the three numerators,

$$|q_0(1+z^{-1}+z^{-2}+\ldots+z^{-n})|$$
$$\leq q_0(1+|z^{-1}|+\ldots+|z^{-n}|)=q_0(n+1) \tag{32}$$

Dividing (30) by $f_1(z^{-1})f_1^*(z^{-1})$

$$\Gamma_n(z^{-1})\Gamma_n^*(z^{-1})=1-\mu^2/f_1(z^{-1})f_1^*(z^{-1}) \tag{33}$$

(31) indicates a maxmum value. Also $f_1(z^{-1})f_1^*(z^{-1})$ reaches a maxmum due to (30). As a result, (33) gives the value which is the closest to 1. Represented by $-10\log\Gamma_n(z^{-1})\Gamma_n^*(z^{-1})$, the attenuation of the discrete transmitted frequency components is the minimum in the frequency characteristics of the proposed coupled-line type multipliers

VI. Discrete Frequency Components of a Train of Gaussian Pulses

Let v(t) described in II.(ii) be a Gaussian pulse. Then, the Fourier transform of v(t) is also Gaussian, and (3) can be given by

$$v(t)=\left\{\frac{1}{2\pi(\Delta t)^2}\right\}^{1/4}\exp\left\{-\left(\frac{t}{2\Delta t}\right)^2\right\} \tag{34a}$$

$$V(\omega)=\left\{\frac{2\pi}{(\Delta\omega)^2}\right\}^{1/4}\exp\left\{-\left(\frac{\omega}{2\Delta\omega}\right)^2\right\} \tag{34b}$$

where Δt and $\Delta\omega$ are called effective duration and effective bandwidth. It is known that more than 99.7% of total energy is included in the range of $|t|<3\Delta t$ or $|\omega|<3\Delta\omega$. In the case

of a Gaussian pulse, from the uncertainty relation [9],[10] (See Appendix),

$$\Delta t \cdot \Delta w = 0.5 \tag{35}$$

Because of

$$\int_{-\infty}^{\infty} | v(t) |^2 dt = 1,$$

the total energy of (34) is 1.

The Fourier series expansion and its Fourier transform to a train of Gaussian pulses can be obtained by substituting (34) into (6) or (11). As seen from (34), the Gaussion pulse could not be called a time-limited pulse waveform in a strict sense. However, assuming both the edges of the waveform represented by (34) reach zero, so that no overlap occurs with adjacent pulses, we can acknowledge following equations with respect to (6a) and (11a):

$$\int_{-T/2}^{T/2} | v_{Tr}(t) |^2 dt = 1$$

$$\int_{-T/2}^{T/2} | w_{Tr}(t) |^2 dt = 1$$

The energy spectra of input pulse trains are given by multiplying the periods by the mean power of periodical pulses. Therefore:

(a) in the case of a train of unipolar Gaussian pulses

$$\frac{\sqrt{2\pi}}{T\Delta\omega} \sum_{k=-\infty}^{\infty} \exp\{-(k\omega^+/\Delta\omega)^2/2\} = 1 \tag{36a}$$

(b) in the case of a train of bipolar Gaussian pulses

$$\frac{\sqrt{2\pi}}{T\Delta\omega} \sum_{k=-\infty}^{\infty} \exp[-\{(2k+1)\omega^+/2\Delta\omega\}^2/2] = 1 \tag{36b}$$

However, (36b) is obtained by multiplying the half-period T by the mean power. The energy spectra are also discrete and given by each term of the left sides of (36) [See Fig.9(b) and Fig.10(b), where negative components are omitted].

In Fig.8(a) of[2], the pulse width generated by P. G. was arround 1.1nsec. Assuming a train of Gaussian pulses with period $T = 5.2$nsec, fundamental frequency $f^+ = 192$MHz and pulse width $3\Delta t = 0.55$nsec, as shown in Fig.5, almost all the energy (99.63%) of the Gaussian pulse train concentrates within $3\Delta f$. Here, $3\Delta f = 1.3$GHz gue to (35). Figs.9(a)(b) indicate the frequency characteristics of the test circuit A of [2], and the energy spectrum of Fig.5. In Fig.9(b), f0 indicates the direct current(DC) component and $f1 = f^+$, $f2 = 2f^+$, . . .hold. For the design of proposed multipliers, it is desirable that the frequency characteristics are satisfied in the region of 0−1.3GHz. As seen from Fig.1 in [2], test circuit A is a directional coupler, which cuts off the DC component completely. The frequency components f2, f4,. . . in Fig.9(b) are rejected, and others f1,f3,. . . transmit to output port A_2, In this way, output pulses can be formed twice as fast as input.

Similar arguments are valid in test circuit B in [2]. Figs.10(a)(b) show the frequency characteristics of test circuit B, and the energy spectrum of Fig.6, respectively. As seen from (36b), the DC component is not included in the train of bipolar pulses. Comparing both figures, it is understandable that f1,f3,f4,...are rejected and f2,f5,... penetrate to output port B_2. Higher frequencies than f5 can safely be neglected. According to the consideration from the frequency domain, it can be said that most of the waveform in Fig.8(c) of [2] comes from the transmitted discrete frequency component f2. The pulse width being shortened, the frequency domain spectra spread to higher bands.

As a result, the continuous waveform in Fig.8(c) of [2] is separated into single pulses.

Referring back to Fig.8, the frequency characteristics have two different peak values in a period: for a chain line, one is at $f/f_0=1$, and the other is at $f/f_0=0$ (or $=2.0$). The same thing can be said in Fig.10(a). The verification in section V ensures that attenuation of the transmitted components is a minimum even if the frequency characteristics have different peak values within a period.

VII. Conclusions

A train of periodical impulses consists of equi-amplitude equi-spacing discrete frequency components. On the other hand, in case of a train of periodical pulses, it possesses the same discrete frequency components as that of impulses, but the amplitudes are different and are given by the Fourier transform of the constituent single pulse waveform. Therefore, generally, as the frequency is increased, the amplitudes are close to zero. Regarding the input pulses generated by the pulse generator as Gaussian pulses of duration 1.1nsec, the frequency band where almost all the energy of the train of Gaussian pulses concentrates is 0−1.3GHz. This fact means that the distributed coupled-line networks can be used as digital frequency multipliers even if the specified frequency characteristics are damaged in the higher frequency region.

In section III, functions of coupled-line type multipliers have been explained, and it has been shown that a coupled-line type multiplier works as a kind of a passive filter which eliminates certain discrete frequency components and transmits other components to the output port. As a result, the transmitted components from a train of output pulses with a higher repetition frequency than the input one in the time domain.

In section IV and V, it has been proved that attenuation of the transmitted components is the minimum.

The proposed multipliers have the dratback of lowering amplitude level and need amplitude amplifiers for actual use. Or, a train of higher amplitude level pulses should be input in advance in order to have necessary output level. However, it could be said that the multiplication by passive elememts only would be worthy of note.

In part II, which will be presented in the near future, energy ratio at a specified frequency and computer output Simulation will be demonstrated with respect to Cosine half wave inputs.

Appendix[9]
The Definition of Δt and $\Delta\omega$

Under the condition of $\int_{-\infty}^{\infty} t\,|\,v(t)\,|^2 dt=0$,

$$(\Delta t)^2 \triangleq \int_{-\infty}^{\infty} t^2\,|\,v(t)\,|^2 dt \tag{A.1}$$

$$(\Delta\omega)^2 \triangleq \frac{1}{2\pi}\int_{-\infty}^{\infty} \omega^2\,|\,V(\omega)\,|^2 d\omega \tag{A.2}$$

Uncertainty Relation

$$\Delta t\cdot\Delta\omega \geq 0.5 \tag{A.3}$$

References

[1] I.Sakagami, N.Miki, N.Nagai, and K.Hatori, "Digital frequency multipliers using multisection two-strip coupled line," IEEE Trans. Microwavee Theory Tech., vol.MTT-29, pp.118–122, Feb. 1981.

[2] I.Sakagami, N.Nagai, and K.Hatori, "On Reducing the Period of Input Pulse Train Using Coupled-Line Networks," IEEE Trans. Microwave Theory Tech., vol.MTT–35,pp.409–414, April 1987.

[3] L.J.P.Linner, "Time domain analysis of commensurate distributed-line networks," IEEE Trans. Circuit Syst., vol.CAS–22, pp.334–343, April 1975.

[4] B.P.Lathi, *Communication Systems*. New York:Wiley, 1977, ch.1.

[5] G.F.Ross, "The transient analysis of certain TEM mode four-port networks," IEEE Trans. Microwave Theory Tech., vol.MTT–14, pp.528–542, Nov. 1966.

[6] A.Gersho and B.Kinariwara, "A systhesis algorithm for cascaded transmission lines", in Proc. 6th. Ann. Allerton Conf. on Circuit and Systems Theory, pp.889–897, Oct. 1968.

[7] K.A.Boakye and O.Wing, "On the time-domain realizability conditions for cascaded transmission-line networks," IEEE Trans. Circuits Syst., vol.CAS–21, pp.387–391, May 1974.

[8] K.Kurokawa, "Power waves and the scattering matrix," IEEE Trans. Microwave Theory and Tech., vol.MTT–13, pp.194–202, Mar. 1965.

[9] T.Hosono, *Fundamentals of Information Engineering*. Corona Publishing, 1970.(in Japanese)

[10] A.Papoulis, *The Fourier Integral and Its Applications*. New York, McGraw-Hill, 1962.

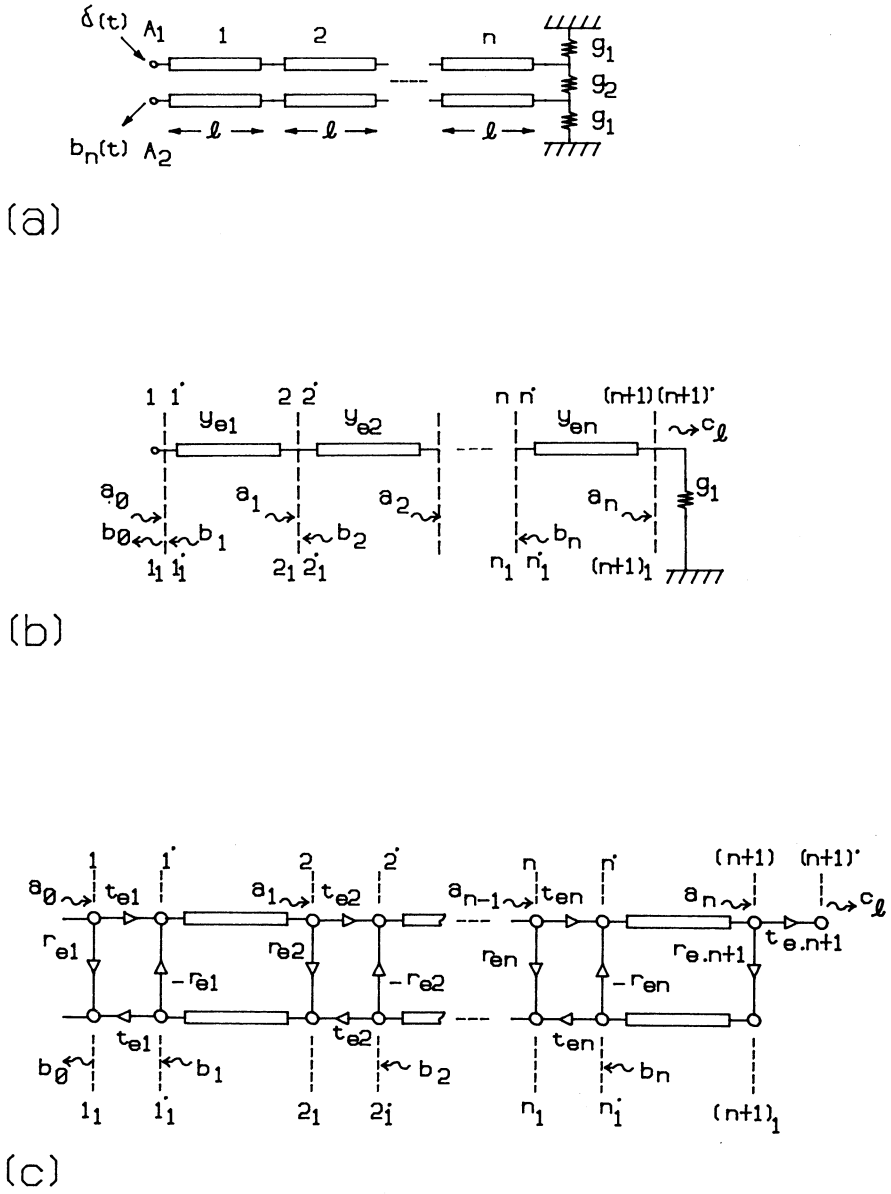

Fig. 1 (a) A constant-resistance n-section coupled-line network.
(b) An even mode equivalent circuit.
(c) An equivalent signal flow graph.

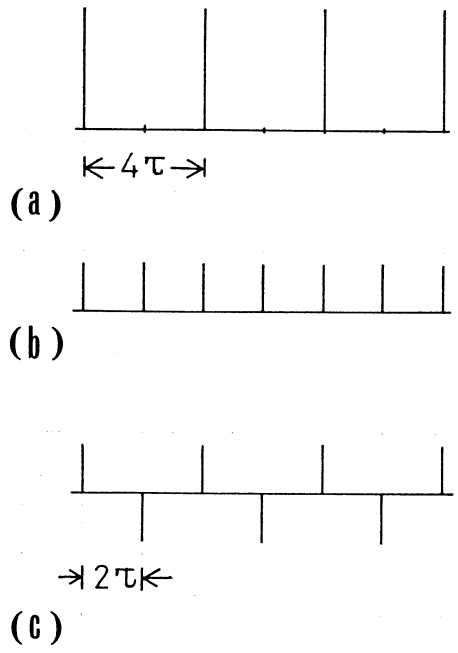

Fig. 2 Input/output responses in case of n=1.
(a) A train of input unipolar impulses.
(b) Output unipolar impulses - In case of Section III(i).
(c) Output bipolar impulses - In case of Section III(ii).

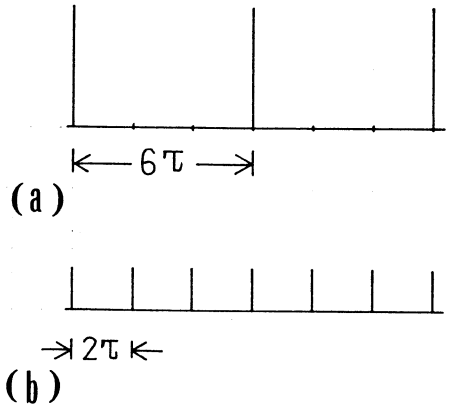

Fig. 3 Input/output responses in case of n=2.
(a) A train of input unipolar impulses.
(b) Output unipolar impulses - In case of Section III(i).

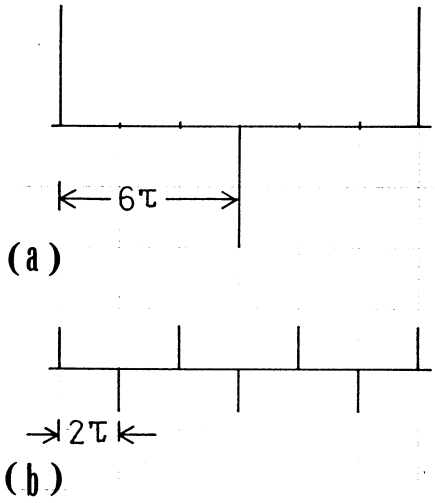

Fig. 4 Input/output responses in case of n=2.
(a) A train of input bipolar impulses.
(b) Output bipolar impulses - In case of Section III(iii).

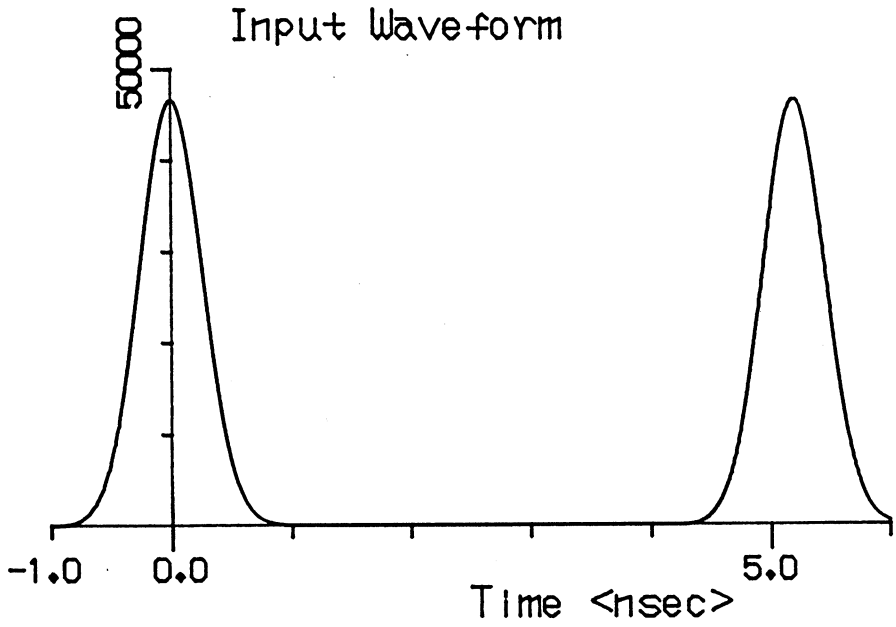

Fig. 5 A train of unipolar Gaussian pulses.

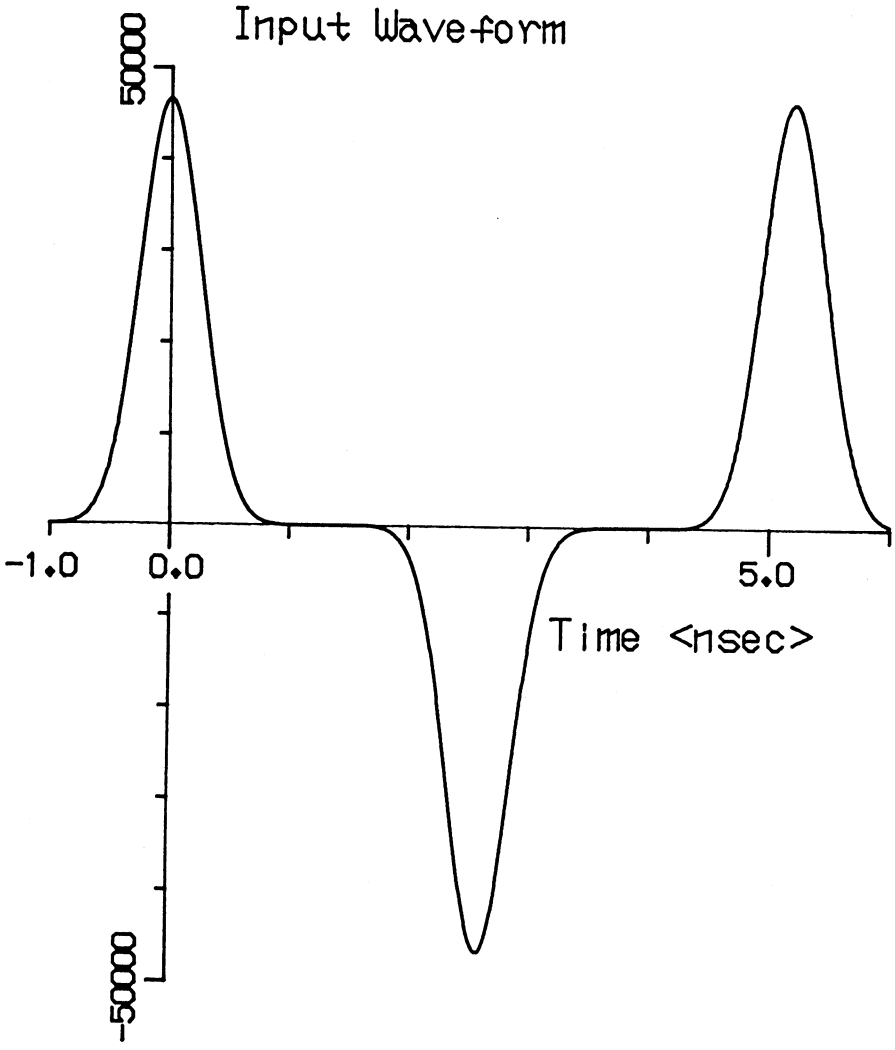

Fig. 6 A train of biplolar Gaussian pulses.

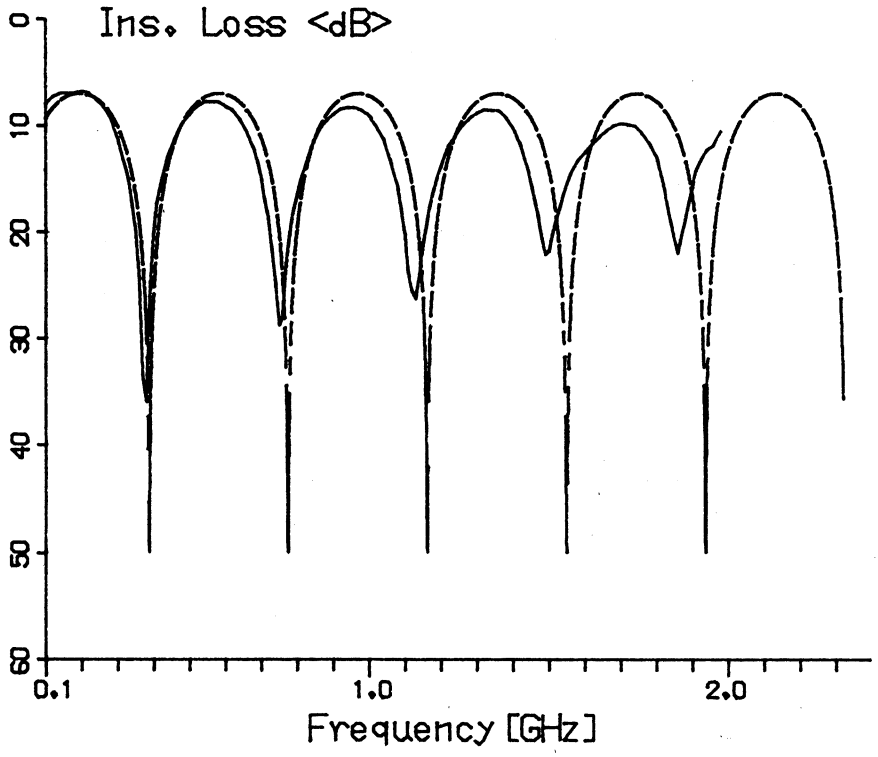

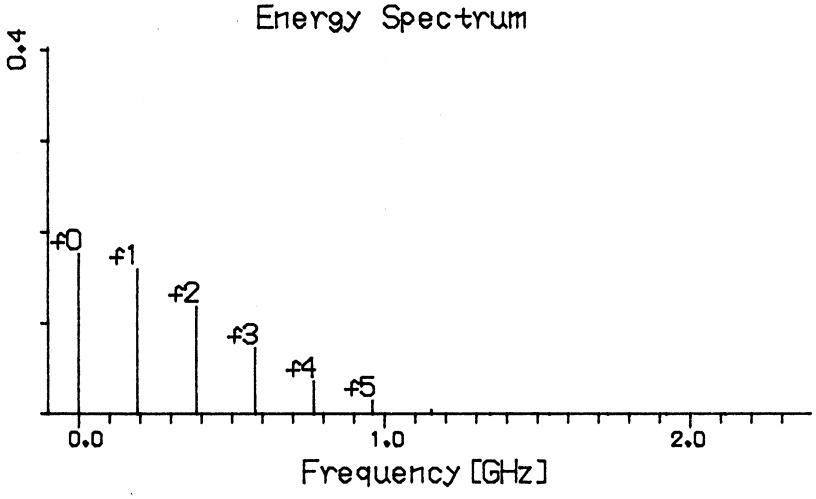

Fig. 9 (a) Frequency characteristics of the test circuit A in [2].
Solid line : measurement. Broken line : theory.
(b) Energy spectrum of input pulse train in Fig. 5.

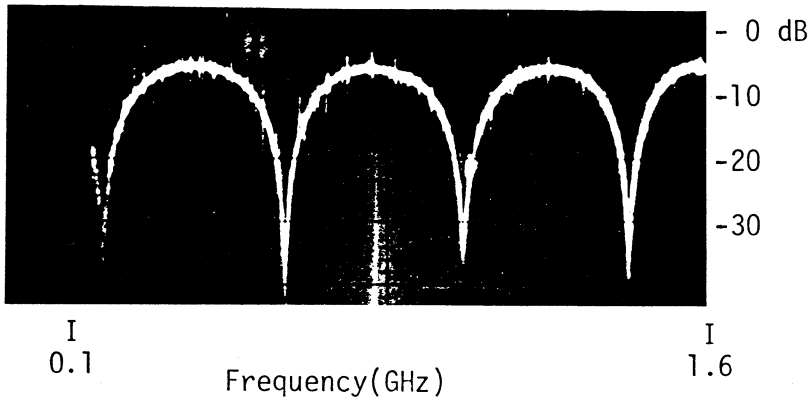

Fig. 7 A photograph of the transmitted frequency characteristics of Fig. 9 in [1].

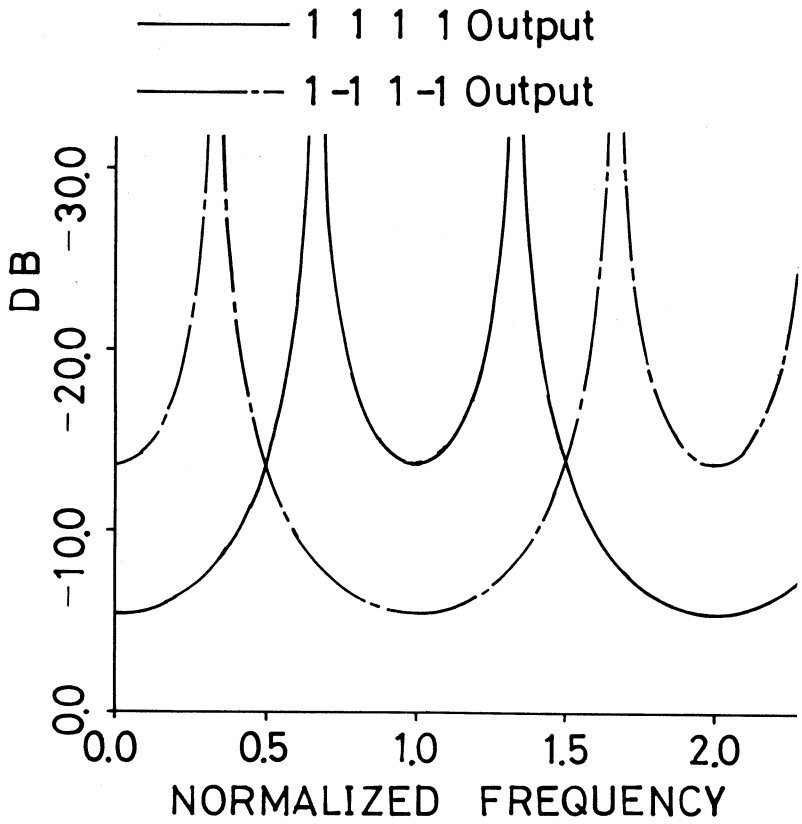

Fig. 8 Theoretical frequency characteristics of the 2-section coupled-line digital frequency triplers. $r_{el}=0.2$.
The solid line : case of III(i). The chain line : case of III(iii).

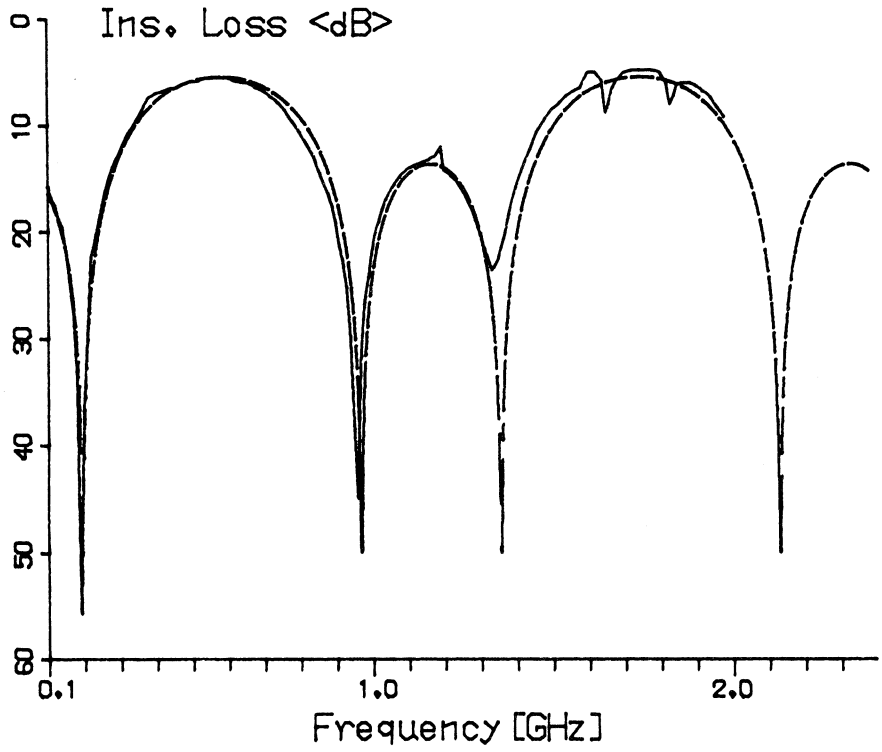

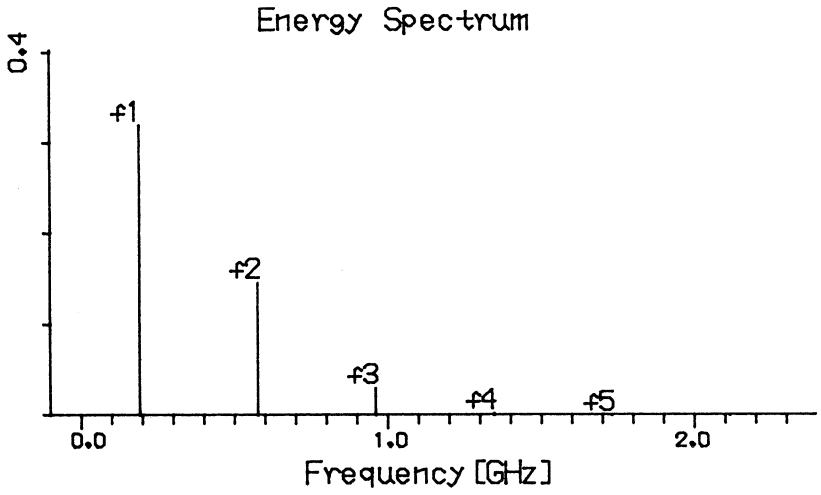

Fig. 10 (a) Frequency characteristics of the test circuit B in [2].
Solid line : measurement. Broken line : theory.
(b) Energy spectrum of input pulse train in Fig. 6.